Cloud Thickness Estimation from GOES-8 Satellite Data Over the ARM-SGP Site

V. Chakrapani, D. R. Doelling, and A. D. Rapp
Analytical Services and Materials, Inc.
Hampton, Virginia

P. Minnis
National Aeronautics and Space Administration
Langley Research Center
Hampton, Virginia

Introduction

The effects of clouds on radiative forcing are topics of intense interest and of direct relevance to climate change. They remain the greatest source of uncertainty in global climate models. There are many cloud properties that can alter the effect of clouds on the climate system. One such key parameter is the cloud thickness that affects the distribution of radiative cooling within an atmospheric column. Algorithms and models that explicitly include cloud base and cloud thickness to compute the radiative parameters typically rely on crude assumptions such as constant cloud thickness. Cloud top heights are routinely derived from satellite data; however, obtaining cloud base is not as straightforward. Minnis et al. (1990) and Smith et al. (1992) developed methods for inferring the physical thickness of cirrus clouds by correlating it with cloud optical depth and cloud effective temperature. Minnis et al. (1992) found a strong correlation between the square root of cloud optical depth and thickness for marine stratocumulus clouds. These earlier techniques were combined and used for cloud thickness retrieval for Atmospheric Radiation Measurement (ARM) Program (Minnis et al. 1995). Because these methods are based on very limited datasets taken during field experiments, their accuracy and applicability are highly uncertain. With the availability of continuous lidar, radar, ceilometer, and satellite retrievals over the ARM Southern Great Plains (SGP) Central Facility (CF), it is possible to develop and test cloud thickness retrieval methods using a wider variety and better sampling of cloud conditions than heretofore possible. In this study, empirical models for four single-layer cloud types are developed by correlating satellite-derived microphysical properties with cloud thickness data derived from active instruments at the ARM CF between March and December 2000. The resulting empirical model performance is then compared to that of the earlier parameterization.

Data and Methodology

Visible (0.65 µm, VIS), solar-infrared (3.9 µm, SIR), infrared (10.8 µm, IR), and split-window channel (12.0 µm, SWC) data taken half hourly from the eighth Geostationary Operational Environmental Satellite (GOES-8) at a nominal 4-km resolution were analyzed and averaged on a 0.5° equal angle grid, centered over the ARM SGP site (Minnis et al. 2002). Vertical profiles of temperature and humidity

were obtained by interpolating the 60-km resolution ARM-Rapid Update Cycle (RUC; Benjamin et al. 1994) products to match the current analysis grid and image times. The RUC surface air temperature was used to estimate the surface skin temperature (T_s). Daytime pixel-level cloud properties of optical depth (τ), IR emissivity (ε), cloud radiating temperature (T_c), phase (ice or water), particle size in terms of effective radii for water (r_e) or effective diameter for ice (D_e), and ice water path (IWP) or liquid water path (LWP) are computed using the Visible-infrared Solar-infrared Split-window Technique (VISST) described in Minnis et al. (2002). The cloud effective height (Z_c) is determined by matching T_c with the corresponding RUC temperature profile. The cloud emissivity has been taken into account in the derivation of T_c from the IR channel. Z_c is often close to the actual cloud-top height when the cloud is optically thick. Days when the ground was covered with snow were eliminated from the analysis, since the optical depth may be enhanced by the brighter-than-normal surface. Surface observations from nearby Ponca City and Enid Automated Surface Observing System (ASOS) stations along with GOES-8 satellite visible images were used to identify days with snow cover. Only data with a solar zenith angle of 77° or less were used in this analysis. Only cases with satellite cloud coverage greater than 95% are used to insure that broken clouds were eliminated from the analysis. In addition, mixed-phase cloud cases were not considered in this study. The standard deviations of the cloud properties are computed from the ~169 pixels in the 0.5° region.

The sgparscl1clothC1 product over the ARM SGP CART site for the same time period March - December 2000 was extracted from ARM archive. The CloudBaseBestEstimate (best estimate) is used for cloud-base height, and is a composite of ceilometer, Micropulse Lidar (MPL), and Millimeter Cloud Radar (MMCR) data. If the best estimate was not available, because both the ceilometer and MPL data was missing, the CloudLayerBottomHeightMPLCloth (E. E. Clothiaux, personal communication) was used. The latter algorithm combines both the MMCR and MPL data, but in this situation, only the radar is used for cloud base determination. In either case, no cloud base is given if the cloud is precipitating enough to cause suspect base heights. In-house validation of the cloud base heights, during precipitation, showed good agreement between the nearby ASOS stations, best estimate, and the Clothiaux cloud base heights. On rare occasion, when the Clothiaux cloud base was used, the Clothiaux "insect clutter algorithm" detected insects instead of the low clouds, for example on May 22, 2002. If visual satellite imagery inspection and nearby ASOS stations confirm low clouds on those days, they were removed. The CloudLayerTopHeigthMplCloth is used for the cloud top height, and cloud thickness (Δz) is the difference between the cloud top and base. The Δz was averaged over 20-minute intervals centered at the GOES-8 satellite image times. The radar data used for the analysis were required to have continuous cloud coverage for 20 minutes and only single layer homogeneous clouds, as identified by the number of layers in the Clothiaux algorithm.

The merged cloud property and thickness data set was first divided into ice and water clouds. Correlation coefficients (r) were then computed for all the cloud properties and their standard deviations (σ) with cloud thickness. Overall, the natural logarithm of τ had the greatest correlation with thickness. Plots of $\ln(\tau)$ and thickness were examined for each phase. Figure 1 indicates that water clouds have a bimodal distribution. The water clouds are classified as (optically) thick and thin stratus and are separated by $\tau<10$ and $\sigma(\varepsilon) >0.1$ for thin stratus. Note, $\sigma(\varepsilon)$ is very small for $\tau >10$. For optically thin ice clouds there is a slightly better correlation with τ rather than $\ln(\tau)$. Ice clouds were classified into cirrus (optically thin and low emissivity) by $\tau<10$ and $\varepsilon<0.95$ and the remaining cases are cumulus or cumulonimbus. After the data were classified into cirrus, cumulus, thick and thin stratus, the correlation

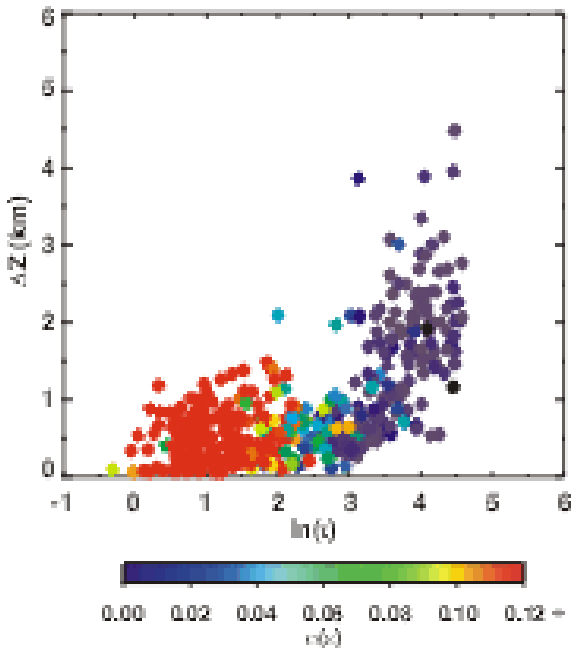

Figure 1. Scatter plot of ln(τ) and Δz for water clouds. Points are color coded, with respect to σ(ε).

coefficients of various cloud properties were computed for each cloud type to determine their significance and are shown in Table 1. Statistically significant parameters are then used for constructing the empirical model.

Table 1. The correlation coefficients of various GOES-8 retrieved cloud properties with surface-based cloud thickness (Δz) for the cloud categories used in this study. The cloud property standard deviations are shown in red.

	t	**LWP or IWP**	Z_c	r_e **or** D_e	T_c	e	**ln(t)**	#
Cirrus	0.72	0.72 0.45	0.25 -0.36	0.13 -0.39	-0.43 -0.38	0.66 -0.27	0.68	65
Cumulus	0.70	0.68 0.55	0.40 0.03	0.18 0.13	-0.27 0.03	0.57 -0.44	0.81	141
Thick stratus	0.65	0.62 0.49	0.39 0.01	0.23 0.18	-0.33 0.20	-0.21 -0.35	0.66	209
Thin stratus	0.16	0.08 0.05	0.07 -0.07	-0.19 -0.12	-0.20 -0.07	0.21 -0.07	0.20	208

Results

For each cloud type, a stepwise multiple regression approach is taken. Each of the cloud properties is evaluated until there is no significant improvement in r^2 with thickness. An example of cirrus-cloud radar reflectivity over the SCF is shown in Figure 2a. The best estimate and Clothiaux cloud base and top heights are superimposed on the radar images. For the cirrus category the cloud properties of τ and IWP have a similar r = 0.72, an expected similarity because IWP depends on τ and D_e. Although σ(T_c)

is nearly uncorrelated with Δz directly, in conjunction with τ, it is statistically significant. Figure 2b illustrates that smaller values of $\sigma(T_c)$ are mostly associated with cases having actual values of Δz greater than would it be obtained from the linear regression with τ. For the cirrus case the final equation is given by,

$$\Delta z = 1.038 + 0.779 \cdot \tau - 0.146 \cdot \sigma(T_c) + 0.014 \cdot D_e.$$

The root mean square (rms) error is 0.84 km with $r^2 = 0.66$. The individual cloud property contributions are 78.5%, 17.8% and 3.6% for τ, $\sigma(T_c)$ and D_e respectively.

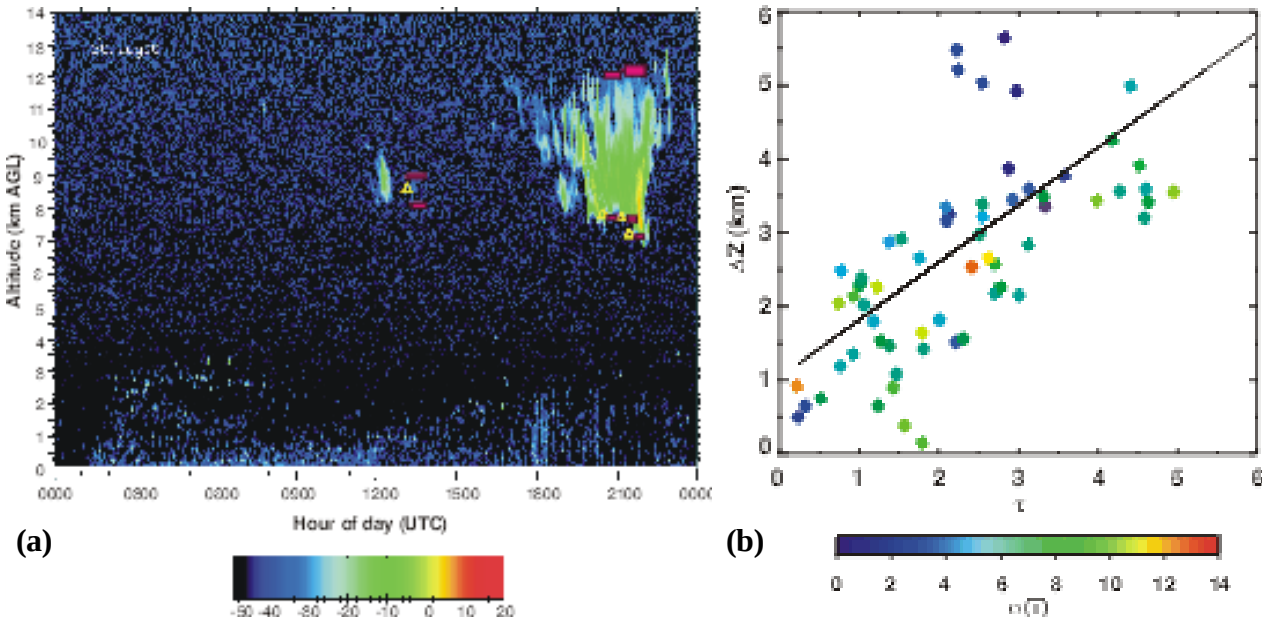

Figure 2. (a) Radar reflectivity in dbz of a cirrus cloud on August 30, 2000. Yellow triangles represent the cloud base best estimate and magenta lines the Clothiaux cloud base and top. (b) Scatter plot and regression line of τ and Δz for cirrus. Points are color coded with respect to $\sigma(T_c)$.

Similar analyses were carried out for the cumulus data. Figure 3a shows a radar image of a typical deep convective cloud. For cumulus clouds, $\ln(\tau)$ has the best correlation with Δz. The greatest value of r given in Table 1 is probably due to the fact that cumulus clouds have the greatest dynamic range of Δz. No other cloud properties added any significance to the linear regression equation. Thus, for the cumulus type,

$$\Delta z = 1.7061 + 1.8834 \cdot \ln(\tau).$$

The rms error is 1.26 km and r^2=0.662 and the regression is shown in Figure 3b. Precipitating cumulus clouds have a mean thickness of 9.32 km compared with 6.92 km for non-precipitating cumuli (Figure 3b). It is likely that the additional thickness was required to initiate the precipitation. The mean cloud base height was 1.13 and 4.23 km for precipitating and non-precipitating respectively.

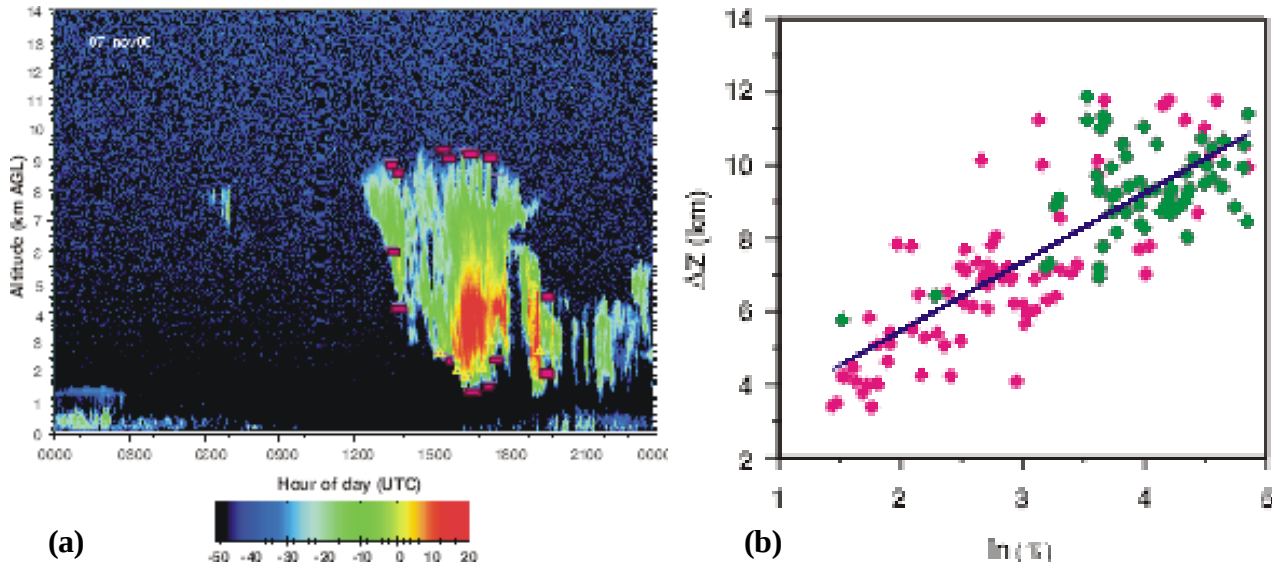

Figure 3. (a) Same as Figure 2a, except for a cumulus cloud on November 7, 2000. (b) Scatter plot and regression line of ln(τ) and Δz for cumulus. The green points are precipitating clouds, whereas the magenta points are not.

For thick stratus clouds, Figure 4a shows a typical radar image for March 18, 2000 over SGP site. Note the position of the cloud base. Generally, the cloud base of stratus clouds in this study are nearly at ground level at 0.61 km, indicating that cloud top height and thickness tend to be correlated. Although T_c and Z_c are correlated with Δz, Z_c is not used in the formulation because it is estimated from T_c using an atmospheric temperature profile. The dataset is limited to a few days and may not represent all stratus clouds during an annual cycle at the CART site. The multiple regression equation for thick stratus is

$$\Delta z = 0.97 \cdot \ln(\tau) + 0.16 \cdot \sigma(T_c) - 2.33.$$

The rms error is 0.61 km and r^2=0.49 for the regression shown in Figure4b. The $\sigma(T_c)$ is greater for greater values of Δz. The individual cloud property contributions are 89.5% and 10.5% for ln(τ) and $\sigma(T_c)$ respectively.

For the thin stratus category, there seems to be no significant correlation with τ (Figure1) or any other cloud property in Table 1 with Δz. The greatest values of *r* do not exceed 0.2. Thin stratus cloud properties have high spatial variation, as typified by σ(ε) displayed in Figure 1. Hence, for thin stratus, the mean cloud thickness value of all thin stratus cases of 0.52 km is given, regardless of any cloud property. The rms error is 0.35 km.

The current cloud product algorithm (Minnis et al. 1995) estimates cloud thickness as follows, $\Delta z = 7.2 - 0.024 \cdot T_c + 0.95 \cdot \ln(\tau)$ for T_c <245 K° and $\Delta z = 0.85 \cdot v\tau$ for T_c >275 K° and is linearly interpolated in T_c in between. Each of the cloud categories in this study was compared with the current algorithm. For cirrus the rms error for this study was 0.84 km and for the current algorithm 1.35 km. Similarly, for cumulus the rms error was 1.26 km compared with 3.5 km for the current algorithm, a definite

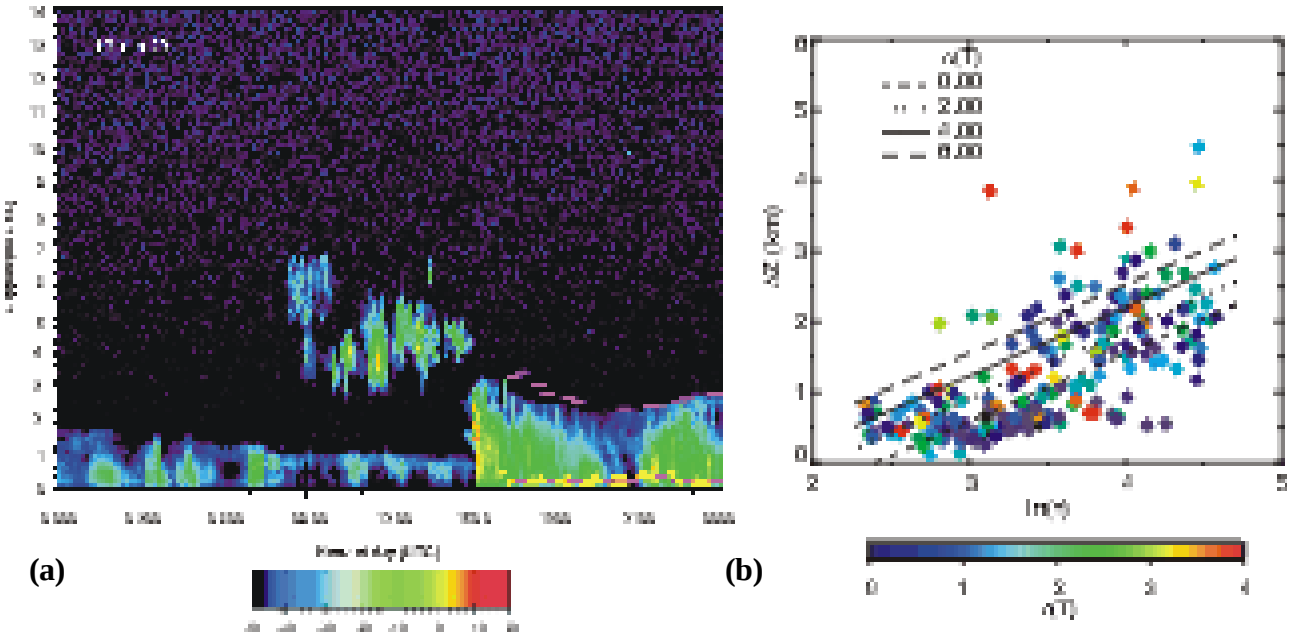

Figure 4. (a) Same as Figure2a, except for a thick stratus cloud on March 18, 2000. (b) Scatter plot and regression lines of ln(τ) and Δz for thick stratus. The regression lines are for differing σ (T_c). Points are also color coded with respect to σ (T_c).

improvement. For thick stratus the rms error was 0.61 km and 0.89 km for this study and the current algorithm, respectively. Even for thin stratus the rms error was 0.35 km and 0.48 km, respectively. As expected, the empirical relationships obtained in this study clearly show considerable improvement over the current formulation.

Summary and Future Work

In this study, GOES-8 cloud property retrievals and cloud thicknesses derived from a combination of radar, lidar and ceilometer data taken over the SCF were analyzed to formulate empirical models for estimating the cloud thickness from cloud property retrievals. The derived parameterizations produce cloud thicknesses that are more accurate than those from previous algorithms. The parameterizations were only applied to the single-layer cloud types considered: thin stratus, thick stratus, deep cumulus, and cirrus. Additional research is needed to ensure that they perform as accurately for independent datasets taken over the SCF as well as over other locations. In addition, they need to be tested for other cloud types like shallow cumulus and altostratus. The current thin stratus formulation with thickness as a constant value is not satisfactory. As more data become available, the thin stratus formulation will be improved to account for variability in the thickness. Nevertheless, the initial results are very encouraging. Thus, the new models will likely be used in future processing of the NASA-Langley cloud property product to estimate cloud thickness.

Acknowledgments

This research was supported by the Environmental Sciences Division of the U.S. Department of Energy Interagency Agreement DE-AI02-97ER62341 under the ARM program. We thank Eugene Clothiaux for useful discussion on estimating the bases of precipitating clouds.

Corresponding Author

Venkatesan, Chakrapani, v.chakrapani@larc.nasa.gov, (757) 827-4691

References

Benjamin, S. G., K. J. Brundage, and L. L. Morone, 1994: The Rapid Update Cycle. Part I: Analysis/Model Description. *Technical Procedures Bulletin No. 416*, NOAA/NWS, 16 pp.

Minnis, P., P. W. Heck, and E. F. Harrison, 1990: The 27-28 October 1986 FIRE IFO Case Study: Cloud parameter fields derived from satellite data. *Mon. Wea. Rev*., **118**, 2426-2446.

Minnis, P., P. W. Heck, D. F. Young, C. W. Fairall, and J. B. Snider, 1992: Stratocumulus cloud properties derived from simultaneous satellite and island-based instrumentation during FIRE. *J. Appl. Meteorol*., **31**, 317-339.

Minnis, P., W. L. Smith, Jr., D. P. Garber, J. K. Ayers, and D. R. Doelling, 1995: "Cloud properties derived from GOES-7 for Spring 1984 ARM Intensive Observing Period using Version 1.0.0 of ARM satellite data analysis program," NASA RP 1366, p.58.

Minnis, P., W. L. Smith, Jr., D. F. Young, L. Nguyen, A. D. Rapp, P. Heck, and M. M. Khaiyer, 2002: Near-real time retrieval of cloud properties over the ARM CART area from GOES data. This Proceedings.

Smith, W. L., Jr., P. Minnis, J. M. Alvarez, P. W. Heck, and T. Uttal, 1992: Estimation of cloud thickness and cloud base from satellite data. *Proceedings of the 11th International Conference on Clouds and Precipitation*, Montreal, Canada, pp.1091-1093.